January 1968
WANL-PR(CCC)-004

Westinghouse Astronuclear Laboratory

ESTIMATION OF MOISTURE FORMATION AND DEPOSITION AND OF THE THRESHOLD FOR TURBINE BUCKET EROSION IN POTASSIUM AND CESIUM VAPOR TURBINES

FINAL REPORT

Astronuclear Laboratory

WANL-PR(CCC)-004

ESTIMATION OF MOISTURE FORMATION AND DEPOSITION AND OF THE THRESHOLD FOR TURBINE BUCKET EROSION IN POTASSIUM AND CESIUM VAPOR TURBINES

FINAL REPORT

January 1968

Union Carbide Order No. 2990

by

T. C. Varljen

C. M. Glassmire

Systems Engineering

INFORMATION CATEGORY:

UNCLASSIFIED

[signature] 3/1/68

Authorized Classifier Date

TABLE OF CONTENTS

I. INTRODUCTION

The Oak Ridge National Laboratory is engaged in a comparative study of cesium and potassium vapor turbine-generator units for space power systems. The Westinghouse Astronuclear Laboratory is providing technical assistance to this work in the form of an analysis of the moisture formation and deposition in four reference turbine designs.

A two-stage and a three-stage cesium vapor turbine, and a five-stage and an eight-stage potassium vapor turbine have been selected for this analysis.

The model which has been employed in this study was developed under the auspices of the National Aeronautics and Space Administration under Contract NAS 7-390. This work is a continuing effort to provide a set of analytical and numerical tools which simulate the gross features of the various mechanisms leading to turbine blade erosion. The model draws on extensive experience with steam turbines and the limited information available in connection with liquid metal vapor machines.

A detailed exposition of the model is given in reference (1). Figure 1 shows schematically the various steps involved in the analysis. For the purposes of this study emphasis has been placed on the classical mode of erosion which is attributed to the mechanical impingement of moisture on rotor blade surfaces. The following summarizes the areas of work which are reported herein:

a) A condensation analysis of the four reference turbines was performed. Estimates were made of the moisture content of the working fluids in each stage and of the size and number distribution of condensate drops.

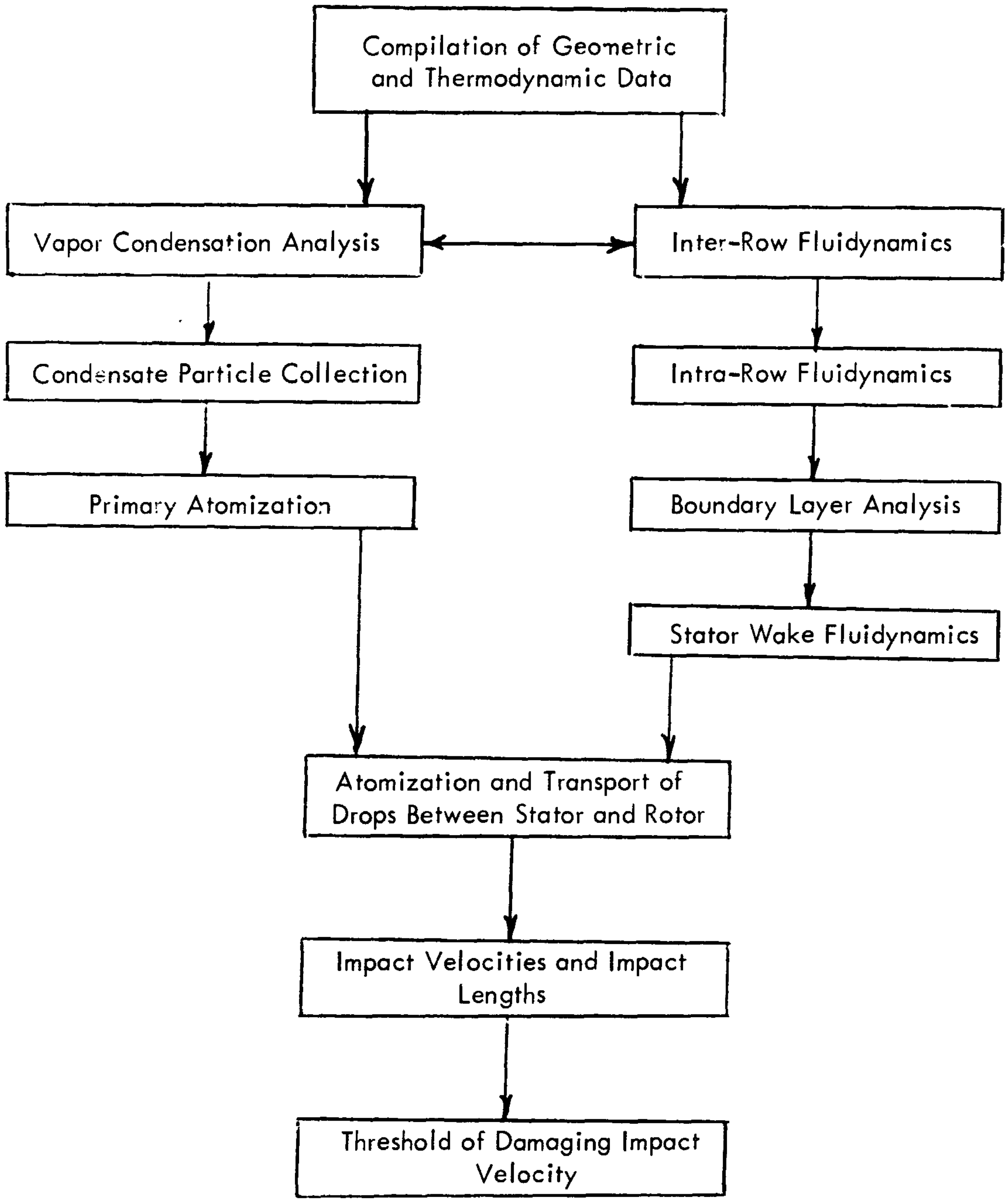

Figure 1. WANL Turbine Blade Erosion Model.

b) Blade contours for each stator row of interest were generated. The last two stator rows of each machine were selected for examination. Using these contours a two-dimensional fluid-flow analysis within the nozzle passages was performed and blade surface velocity profiles generated. Boundary layer characteristics at the stator trailing edges were then estimated.

c) Moisture collection rates were estimated for each stator row.

d) The transport of atomized drops between stator and rotor sections was examined. The detailed interaction of the stator wakes and the atomized liquid was considered. The upper limit of the diameters of impacting drops was estimated.

e) The geometrical aspects of drop impaction on the eight selected rotor blade rows was examined and parametric results obtained for the magnitude of normal impact velocities and the possible extent of eroded regions.

g) The threshold velocities for mechanical erosion of the reference rotor blades was estimated.

2. VAPOR CONDENSATION STUDY

The basic tool in this phase of the analysis is a computer code[2] written by R. E. Kothmann of the Westinghouse Research and Development Center. The function of the code is to analytically predict the condensation point in wet vapor turbines and to determine the moisture content and drop size distributions. The effect of molecular association on the condensation and flow processes is considered.

Several modifications in the code were necessary to meet conditions implied by the ORNL design data. The reference designs assumed inter-stage moisture removal, seal leakage, and vapor bleed for the purpose of regenerative feed heating. The condensation code on the other hand assumed strict continuity between stages. It was not possible to explicity incorporate any provision for moisture losses into the code, however bulk flow rate variations have now been provided for. With the present scheme the desired bulk flow rates entering each stage are used to compute a flow fraction associated with each stator. The inlet axial and relative velocities at each stator are then modified by the appropriate flow fraction. Since the flow area and specific volume are held constant the effect is a reduction in flow rate.

The original code also preserved continuity between blade rows by computing inlet blade angles that were consistent with the inlet specific volume, inlet velocities, and axial flow area. This feature was removed for the present calculations. The inlet blade angles were input and held fixed.

It was found that it was not possible to match the design velocity triangles and pressure ratios using the given turbine configurations. This is not unexpected since an equilibrium calculation was used to establish the original data.

Exit Mach numbers from the nozzle tended to be quite sensitive to small variations in area ratio. It was decided to input a set of desired exit velocities to the code and to arbitrarily decrease exit areas. When a desired velocity was reached in a blade row the appropriate exit area was noted and the calculation for that row terminated. Thus a first pass yielded a set of flow areas and blade heights consistent with the target velocities and the input mean diameters. A subsequent pass with the adjusted blade heights was then made to obtain the condensation results.

The cesium turbines proved quite difficult to analyze because of the supersonic flows involved. To conserve computer time within reasonable limits the condensation calculations were carried to the Wilson Point in each case and an "equilibrium extrapolation" made to predict results in subsequent stages.

2A. TWO STAGE CESIUM TURBINE

This turbine was run with essentially design geometry. It was found that the exit Mach number from the first stator was well below 1.0 so that it was necessary to decrease the flow passage area to increase the flow velocity. This was done by assuming a finite blade thickness (such that the resulting throat-to-exit area ratio was consistent with the desired exit Mach number). This process is not automated and the results are not entirely satisfactory as far as matching the design velocity triangles and pressure ratios are concerned. However it is felt that the droplet size and number estimates are sufficiently insensitive to the velocity and flow area discrepancies and will suffice.

For all of the turbines examined rotor expansions were assumed to be isentropic and a local expansion efficiency of .95 taken for the stators. Inlet conditions for the cesium vapor were as follows:

Total Temperature	$2610^{\circ}R$
Total Pressure	314.6 psia
Vapor Flow Rate	8.24 pps
Quality	20.0° superheat

Table I contains computed values for state points and moisture distribution. Shaft RPM for the cesium machines was 18,000.

Condensation was found to begin just ahead of the first stator throat. The maximum value of nucleation rate was 5.97×10^{19} nuc/ft^3 sec, placing the Wilson Point about 75% of the way through the passage length. The expansion rate at that location was

$$\dot{p} = \frac{1}{p} \frac{dP}{dT} \approx 3600/\text{sec.}$$

Table I. A Summary of the Condensation Analysis Results for the Two-Stage Cesium Turbine

Row	Temperature (^{o}R)	Pressure (psia)	Total Moisture	Mean Droplet Radius (Microns)	Number of Drops/lb
0	2598	310	---	---	---
1S	2278	139	.090	.179	1.3×10^{15}
1R	2266	140	.085	.178	1.3×10^{15}
2S	1790	23.6	.125	.229	1.3×10^{15}
2R	1790	23.6	.169	.253	1.3×10^{15}

Condensation started very close to the nozzle throat and equilibrium was reached rather quickly. The computer program used has difficulties making the subsonic-supersonic transition with any conside . ,le amount of moisture present. We therefore feel that the computed expansion rate is rather low. A value of 10^4/sec is typical for other cesium systems we have examined.(3) As a result the estimates of the mean radii of condensate drops are probably on the high side in this case.

2B. THREE STAGE CESIUM TURBINE

Inlet conditions for the cesium vapor were as follows:

Total Temperature	$2610^{\circ}R$
Total Press e	314.6 psia
Vapor Flow Rate	8.85 pps
Quality	20° superheat

Table 2 lists estimated values for state points, velocities and moisture distribution. Condensation was initiated near the exit of the first stator. The Wilson Point occurred in the vicinity of 98% of the passage length. The maximum value of the nucleation rate was 7.28×10^{20} nuc/ft^3 sec corresponding to an expansion rate of:

$$\dot{p} = \frac{1}{p} \frac{dp}{dT} \approx 8820/sec$$

The above expansion rate appears to be more typical than the rate found for the two-stage turbine. Mean droplet radii of the order of 0.1 μ seem to be characteristic for the last stator of cesium vapor trubines that we have examined.

Table 2. A Summary of the Condensation Analysis Results for the Three-Stage Cesium Turbine

Row	Temperature (°R)	Pressure (psia)	Total Moisture	Mean Droplet Radius (Microns)	Number of Drops / lb
0	2598	310	---	---	---
1S	2262	181	.015	.055	7.3×10^{15}
1R	2353	177	.058	.091	7.3×10^{15}
2S	2070	74	.085	.096	7.3×10^{15}
2R	2070	74	.104	.101	7.3×10^{15}
3S	1790	24	.130	.104	7.3×10^{15}
3R	1790	24	.158	.108	7.3×10^{15}

2C. FIVE STAGE POTASSIUM TURBINE

Stators were assumed to have zero thickness and the rotors a finite central thickness with zero leading and trailing edge thickness. Rotor expansions were assumed to be isentropic as noted and a local expansion efficiency of .95 taken for the stators. Shaft RPM for the potassium machines was 24,000. Inlet conditions for the potassium vapor were as follows:

Total Temperature	$2610^{\circ}R$
Total Pressure	214.3 psia
Vapor Flow Rate	2.29 pps
Quality	20.0° superheat

Table 3 lists computed values for state points, velocities and moisture distribution. Condensation was found to begin near the exit of the second flow passage. The maximum value of the nucleation rate was 2.04×10^{22} nuc/ft^3 sec placing the Wilson point at the exit of the second stator. The expansion rate at that location was:

$$\dot{p} = \frac{1}{p}\frac{dp}{dt} \approx 1 \times 10^5/\text{sec.}$$

The rapid expansion rate produced relatively small estimates for the droplet sizes. The static pressure and temperature at the Wilson Point was 84.2 psia and $2097^{\circ}R$.

The target exit velocities for the third and fourth stators was given as 1643 and 1634 fps. It was not possible to achieve these velocities because of the proximity of the sonic velocity near the exit of both stators. At the exit of the third stator for instance the exit velocity achieved was 1596 fps which is Mach 0.97.

Table 3. A Summary of the Condensation Analysis Results for the Five Stage Potassium Turbine

Row	Temperature (°R)	Pressure (psia)	Total Moisture	Mean Droplet Radius (Microns)	Number of Drops/lb
0	2602	212	---	---	---
1S	2368	146	---	---	---
1R	2367	146	---	---	---
2S	2095	84	5×10^{-4}	.015	2.9×10^{16}
2R	2254	80	.081	.082	2.9×10^{16}
3S	2076	45	.128	.091	2.9×10^{16}
3R	2098	45	.135	.098	2.9×10^{16}
4S	1950	26	.179	.101	2.9×10^{16}
4R	1971	14	.184	.107	2.9×10^{16}
5S	1790	10	.191	.111	2.9×10^{16}
5R	1790	10	.196	.114	2.9×10^{16}

2D. EIGHT STAGE POTASSIUM TURBINE

Stators were assumed to have zero thickness with zero leading and trailing edge thicknesses. Rotor expansions were assumed to be isentropic as noted and a local expansion efficiency of .95 taken for the stators. The shaft RPM was 24,000. Inlet conditions for the potassium vapor were:

Total Temperature	$2610^{\circ}R$
Total Pressure	214.3 psia
Vapor Flow Rate	2.16 pps
Quality	20° superheat

Computed values for state points, velocities and moisture distribution are listed in Table 4. Condensation was found to begin near the exit of the third stator. The maximum value of the nucleation rate was found to be 1.6×10^{20} nuclei/ft^3 sec, corresponding to an expansion rate of 7990/sec. The Wilson Point is apparently right at the exit of the third stator.

The maximum expected condensate particle sizes were found to be $.11\,\mu$ and $.22\,\mu$ for the five-stage and eight-stage potassium turbines respectively. These results are consistent with our experience with other potassium machines.

It should be pointed out that the inlet flow rates listed are for reference only, that is, they are based on the values of inlet vapor velocity input to the condensation code and the computed inlet specific volume of the vapor. For the purposes of estimating condensate collection the design values of flow rate will be used.

Table 4. A Summary of the Condensation Analysis Results for the Eight Stage Potassium Turbine

Row	Temperature (°R)	Pressure (psia)	Total Moisture	Mean Droplet Radius (Microns)	Number of Drops/lb
0	2602	212	---	---	---
1S	2464	171	---	---	---
1R	2464	171	---	---	---
2S	2302	129	---	---	---
2R	2302	129	---	---	---
3S	2142	92	.001	.053	4×10^{15}
3R	2285	91	.067	.151	4×10^{15}
4S	2181	64	.100	.170	4×10^{15}
4R	2195	64	.104	.173	4×10^{15}
5S	2075	43	.121	.180	4×10^{15}
5R	2097	43	.142	.190	4×10^{15}
6S	1969	28	.162	.197	4×10^{15}
6R	1992	28	.179	.203	4×10^{15}
7S	1890	18	.195	.208	4×10^{15}
7R	1890	18	.209	.213	4×10^{15}
8S	1790	10	.222	.218	4×10^{15}
8R	1790	10	.235	.222	4×10^{15}

3. BOUNDARY LAYER FLOW ANALYSIS

Blade Contour Generation

Estimation of turbine blade erosion due to the impact of atomized condensate requires a detailed analysis of the characteristics of the stator blade boundary layer and downstream wake. As a prelude to this it is necessary to generate representative blade contours to facilitate the two-dimensional fluid flow analysis within blade rows. In the present study the stator blades are idealized as infinitely thin foils with a contour in the radial projection which is a quarter ellipse. Appropriate contours for the last and next-to-last stators in each turbine have been generated by the following method.

The basic blade contour in the radial projection is the quarter -ellipse defined by:

$$Az^2 + By^2 + Czy + Dz + Ey = 0 \qquad (1)$$

with the constants:

$$A = 1 + 3\cos^2\phi$$
$$B = 1 + 3\sin^2\phi$$
$$C = -3\sin 2\phi$$
$$D = -4a\sin\phi$$
$$E = -4a\cos\phi$$

The semi-minor axis, a, of the ellipse is given by:

$$a = \frac{L}{\cos\phi + 2\sin\phi} \qquad (2)$$

where L is the axial length of the blade row. The nozzle exit angle, ϕ is fixed at 15°.

The diameter of the passage mean line in the circumferential projection has the following sinusoidal variation from inlet to outlet:

$$\bar{D}(z) = \bar{D}_I + (\bar{D}_o - \bar{D}_I)\sin^2\frac{\pi z}{2L} \qquad (3)$$

In general the effective length of the flow passage is larger than L. A first-order correction to the passage length used in the two-dimensional analysis is made by replacing L in equation (2) by L' which is the arc length computed along the curve (3). This yields:

$$L' = \int_0^L \sqrt{1 + (d\bar{D}/dz)^2} \qquad (4)$$

where:

$$\frac{d\bar{D}}{dz} = \frac{\pi}{L}(\bar{D}_o - \bar{D}_I) \sin \frac{\pi z}{2L} \cos \frac{\pi z}{2L} \qquad (5)$$

Equation (1) is solved numerically for a set of ordinates corresponding to a set of z ranging from o to L'. This yields the lower passage contour. The upper contour is generated by displacing the lower one by the local pitch:

$$y'(z) = y(z) + S(z) \qquad (6)$$

where:

$$S(z) = \frac{\pi \bar{D}(z)}{N_B} \qquad (7)$$

Blade Surface Velocities

The two-dimensional fluid flow analysis was performed with the use of the NASA code 2DINC.[4] The idealized blade with no leading and trailing edge thicknesses cannot be treated by the code. It was therefore necessary to modify each blade contour to accommodate finite leading and trailing edge radii. Values of 30 mils and 5 mils were used for these radii respectively. Surface velocity profiles were completed for the terminal stator of each turbine. Figure (2) is a typical velocity profile drawn for the 7th stage stator of the 8-stage potassium turbine. The surface velocities have been referred to the trailing edge free stream velocity and axial position is referred to the axial blade length.

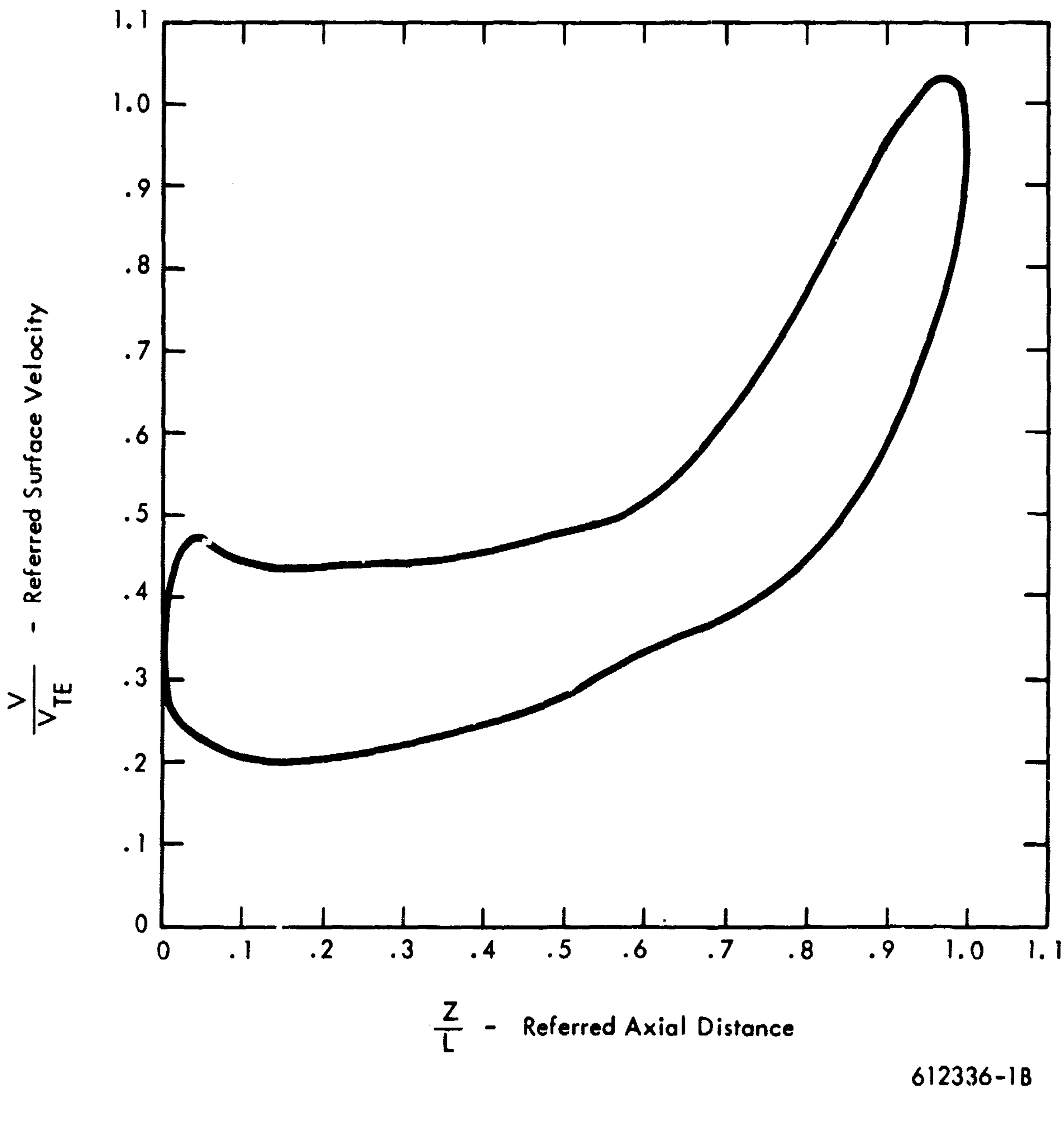

Figure 2. Surface Velocity Profile for the 7th Stage Stator of the Eight-Stage Potassium Turbine.

The velocity profiles generated for the eight stator passages of interest all had the same unconventional shape. The blade sections have a very large solidity, i.e., the chords are large relative to the pitch. Very little turning is accomplished over the leading half of the blades, with most of the velocity increase occurring on the downstream half.

Boundary Layer Characteristics

The evolution of wakes downstream of stator blades was calculated from the boundary layer properties at the trailing edge of blades by the procedure outlined by Lieblein and Roudebush[5]. Starting with estimates of the stator blade surface velocities the Truckenbrodt equation was integrated to yield the required trailing edge properties. A computer program written by W. K. Fentress[6] was used for these calculations. Table 5 summarizes the results of the boundary layer analysis.

Table 5. Trailing Edge Boundary Layer Characteristics

Stator Section	δ_S inches x 10^3	δ_P inches x 10^3	δ_S^* inches x 10^3	δ_P^* inches x 10^3	θ_S inches x 10^3	θ_P inches x 10^3
2Cs - 1S	9.47	2.85	1.57	.344	1.12	.270
2Cs - 2S	14.7	6.82	2.49	.930	1.77	.707
3Cs - 2S	11.3	4.10	1.90	.530	1.35	.408
3Cs - 3S	13.9	3.03	2.80	.362	1.86	.285
5K - 4S	9.40	2.34	1.61	.277	1.14	.218
5K - 5S	9.72	3.73	1.58	.421	1.14	.336
8K - 7S	10.3	4.61	1.62	.586	1.18	.454
8K - 8S	10.3	2.96	1.91	.337	1.31	.268

4. COLLECTION OF CONDENSATE

The deposition of moisture on turbine blade surfaces is considered by examining collection on both the nose and concave face of the blades. The latter collection rate generally dominates. In the present analysis nose radii of .030 inches was assumed for all stators. Negligible collection fractions were associated with the leading edge of these blades.

The collection mechanism is assumed to consist primarily of inertial impaction subject to the macroscopic application of the laws of motion. The computational scheme formulated by W. K. Fentress[(7)] has been used.

Collection rates for the last two stator blade rows of each turbine are summarized in Table 6. Average condensate particle radii were estimated from the condensation analysis discussed above. The moisture collection rates for the two-stage cesium turbine are probably high due to the high estimates of condensate particle size. It is felt that the three-stage turbine results are more characteristic.

Table 6. Estimated Condensate Collection Rates for the Reference Turbine Stator Blades

Blade Row	Mean Drop Radius (microns)	Percent of Bulk Moisture Collected	Bulk Mass Flow Rate (pps)	Row Moisture Collection Rate (pph)
2Cs - 1S	.179	.65	7.39	15.5
2Cs - 2S	.229	3.52	6.03	80.4
3Cs - 2S	.096	.56	7.35	10.4
3Cs - 3S	.104	.50	6.85	14.5
5K - 4S	.101	.91	1.79	9.2
5K - 5S	.110	1.44	1.73	16.9
8K - 7S	.208	3.92	1.70	44.6
8K - 8S	.218	2.38	1.65	30.4

5. TRANSPORT OF ATOMIZED DROPS

The collected moisture is carried along to the rear of the stator vanes by the drag forces of the main vapor stream. The model then assumes that the collected liquid is then detached from the trailing edges of the stator and undergoes a "primary atomization" process. This spray of relatively large drops is caught up and accelerated by the bulk vapor stream or by the decaying wake of the stator. The resulting aerodynamic forces on the large primary drops causes further breakup of most of the drops in a "secondary atomization" process.

The spray of moisture which ultimately impacts the rotors, therefore, will generally consist of a small number of unbroken primary drops (which are potentially the most damaging) and a larger number of secondary droplets. The criterion for breakup of a primary drop is that it exceeds a critical Weber number somewhere along its trajectory. Gardner[8] indicates that the critical Weber number for drop breakup may vary from 13 to 22, depending upon the abruptness of the onset of the aerodynamic drag forces. In the case of potassium and cesium turbines, we find that the onset of these forces is quite abrupt, suggesting the use of 13 as the appropriate critical Weber number.

The Weber number is given by:

$$We_d = \frac{\rho_v (V_{rel})^2 D_d}{\sigma_d} \tag{8}$$

where V_{rel} is the relative velocity of a drop with respect to the local vapor velocity. The Weber number is therefore usually greatest immediately after atomization and then decreases as the drop velocity approaches the stream velocity. Assuming a critical Weber number of 13 drop stability curves were drawn for cesium (Figure 3) and potassium (Figure 4) systems.

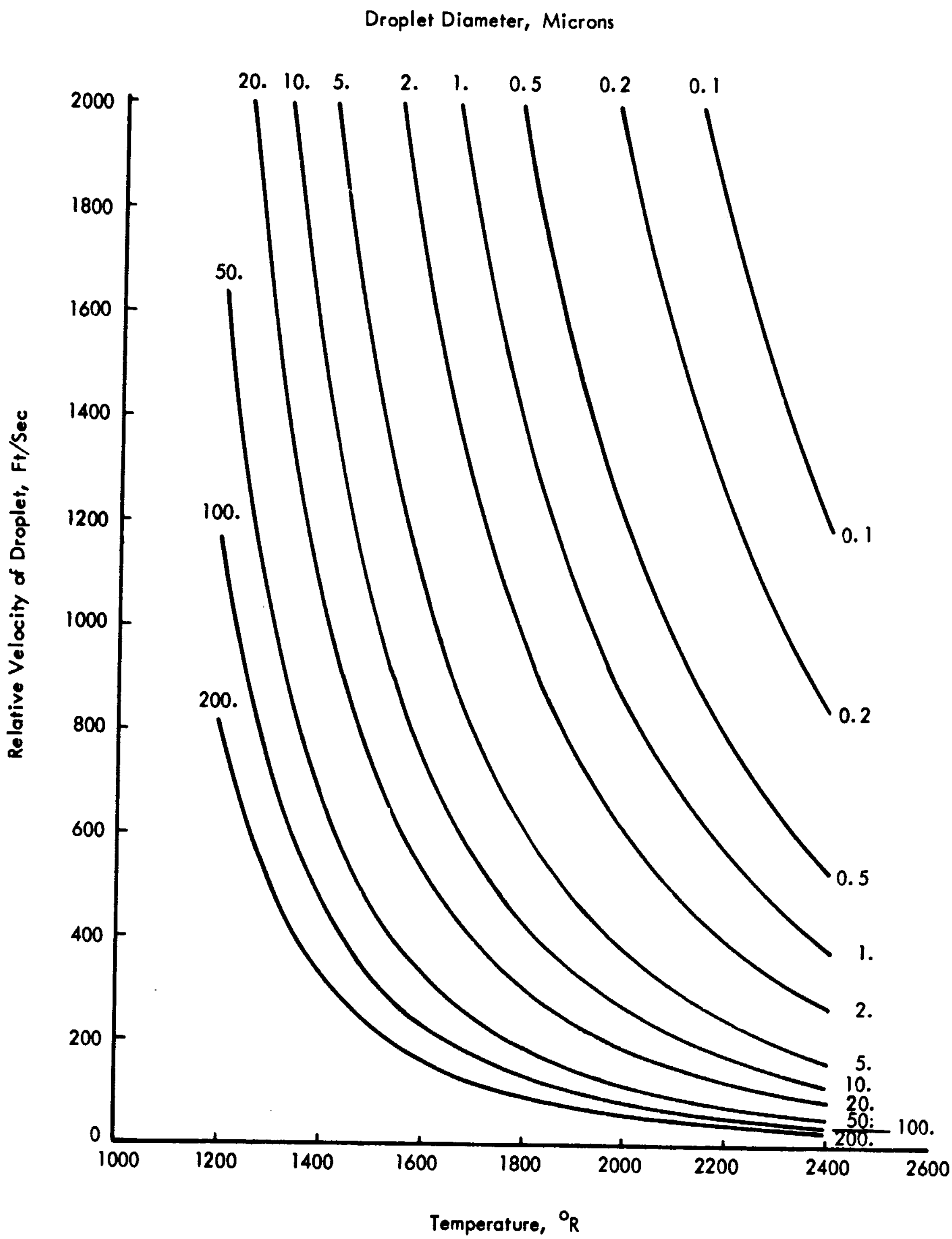

Figure 3. Primary Drop Stability in Cesium Systems

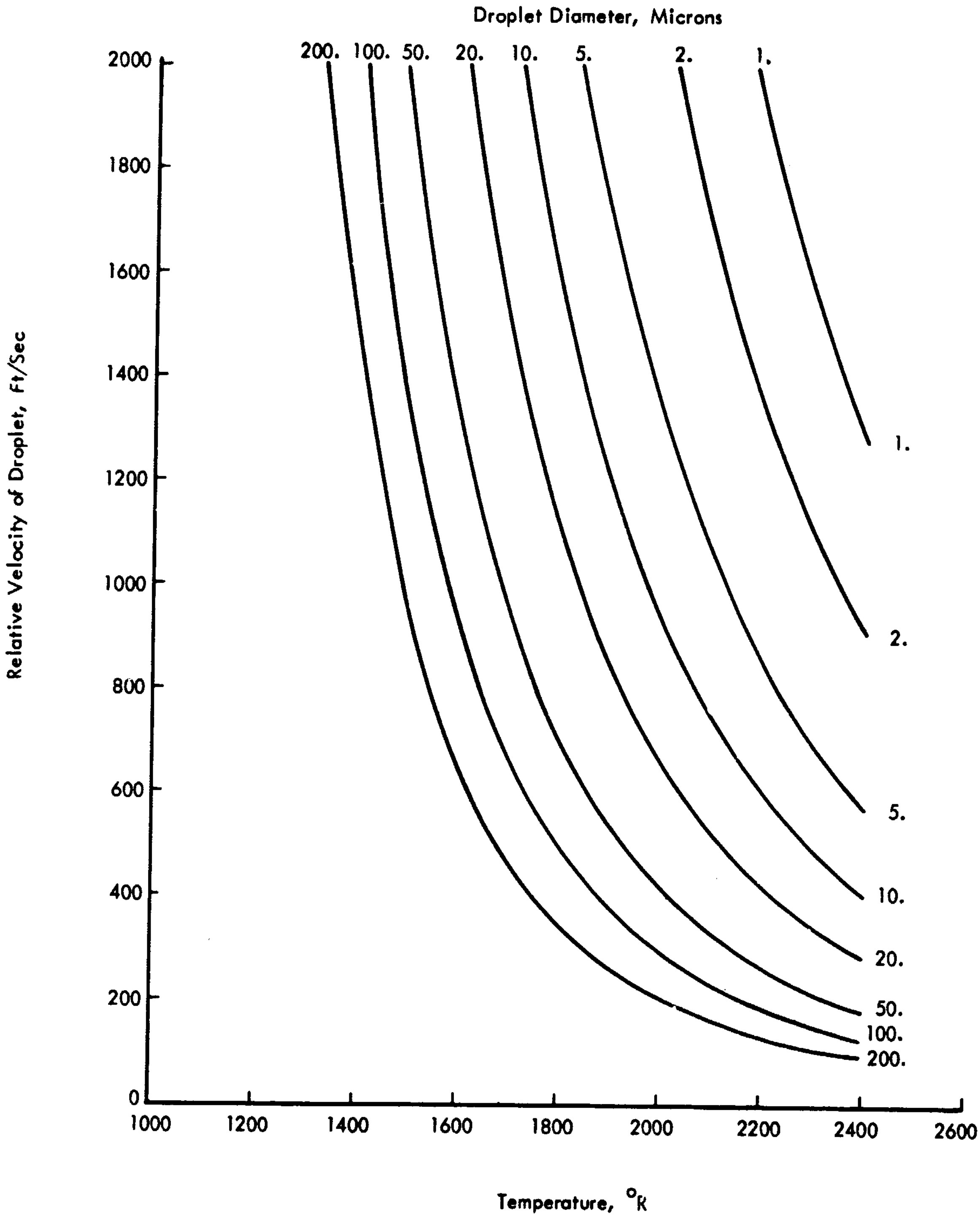

Figure 4. Primary Drop Stability in Potassium Systems

The critical drop velocity is shown as a function of temperature for a typical set of primary drop diameters. A strong temperature dependence is indicated for this process. Consider a 1.0 μ drop diameter in a cesium environment (Figure 3). For velocity-temperature coordinates above and to the right of the 1.0 μ curve the drop will be unstable and will tend to undergo secondary atomization. High temperature systems will tolerate smaller drops than low temperature systems. Cesium systems generally will tolerate much smaller primary drops than potassium systems.

A detailed numerical study of primary drop ballistics was performed for each stator section (the last two stator rows of each turbine). The acceleration of various sizes of drops was examined in the space between stator and rotor planes along two streamlines: the wake axis and the edge of the wake. Drops introduced into the edge of the wake undergo the most rapid acceleration so that only relatively small drops will remain stable. Impact velocities however are correspondingly higher than elsewhere within the wake for drops of the same size. Because of the substantial velocity defect along the wake axis the aerodynamic forces are at a minimum and larger drops will survive to impaction.

Figure 5 illustrates the relationship between initial drop Weber number and drop diameter which is predicted for the four reference turbines. These results depend strongly on the assumed wake characteristics immediately downstream of the trailing edge. If a fixed critical Weber number criteria is used to predict disruption the upper limit of primary drop sizes may be established for each case. Table 7 summarizes the upper limits of stable drop diameters, for the two limiting wake positions, for each turbine. The impact velocity corresponding to each drop size limit is also noted. Since the arrival velocity varies inversely with drop size these are lower velocity limits. A critical Weber number of 13 was assumed. Drops with diameters greater than the limits are expected to break up prior to impact. Figure 6 shows the variation of drop impact velocity with drop diameter for a typical case (the last stator of the five-stage potassium turbine).

Table 7. Limits for the Diameters and Terminal Velocities of Impacting Primary Drops

Turbine Stage	Wake Axis		Wake Edge	
	Drop Diameter (microns)	Impact Velocity (feet/sec)	Drop Diameter (microns)	Impact Velocity (feet/sec)
2Cs - 1	.35	1027.	.16	*
2Cs - 2	3.2	1029.	1.1	1316.
3Cs - 2	1.2	872.	0.5	*
3Cs - 3	3.4	918.	1.6	1104.
5K - 4	9.0	1050.	4.0	1575.
5K - 5	20.	724.	8.0	1331.
8K - 7	19.	663.	8.0	1183.
8K - 8	26.	568.	12.	936.

* The integration scheme used was unstable for small drop diameters.

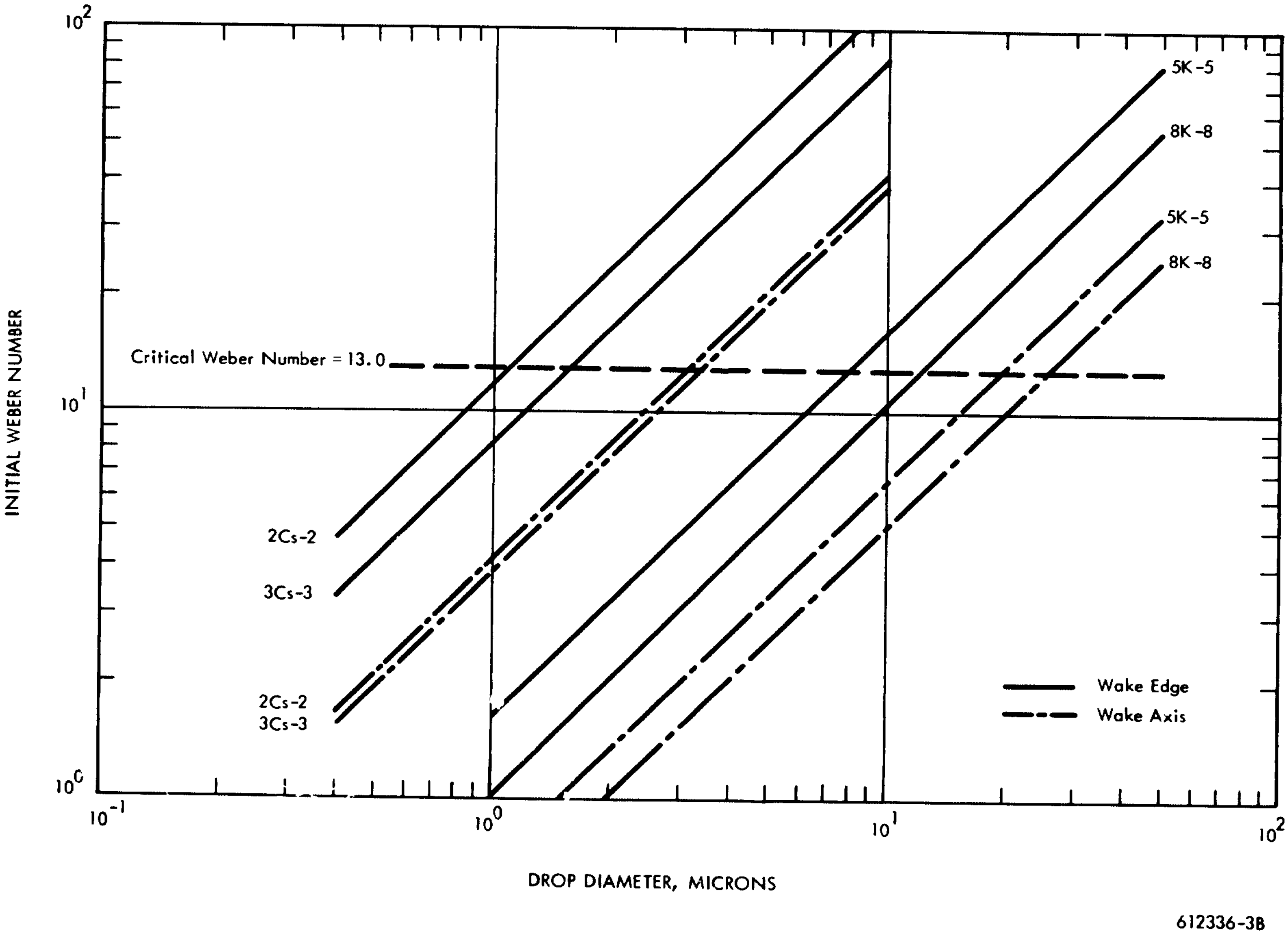

Figure 5. Variation of Weber Number with Drop Diameter for the Reference Turbines.

As expected the cesium turbines are better atomizers than the potassium turbines. The terminal stages of all the turbines characteristically operate at lower temperatures and higher vapor velocities so they generally will have the highest primary drop size limits.

A distance of 0.25 inches has been provided between all stator exit planes and rotor inlet planes. Since the wake axis is inclined (about 75°) with respect to the turbine axis the actual acceleration distance is about 0.97 inches. This distance appears to be adequate to insure that all unstable drops will have sufficient time to complete the secondary atomization process before arrival at the rotor plane. In a recent study[9] we have attempted to provide a closed form estimate of the path length required for an unstable primary drop to disrupt. This distance was found to be of the order of a few drop diameters over the range of Reynolds numbers corresponding to the turbine environments examined here.

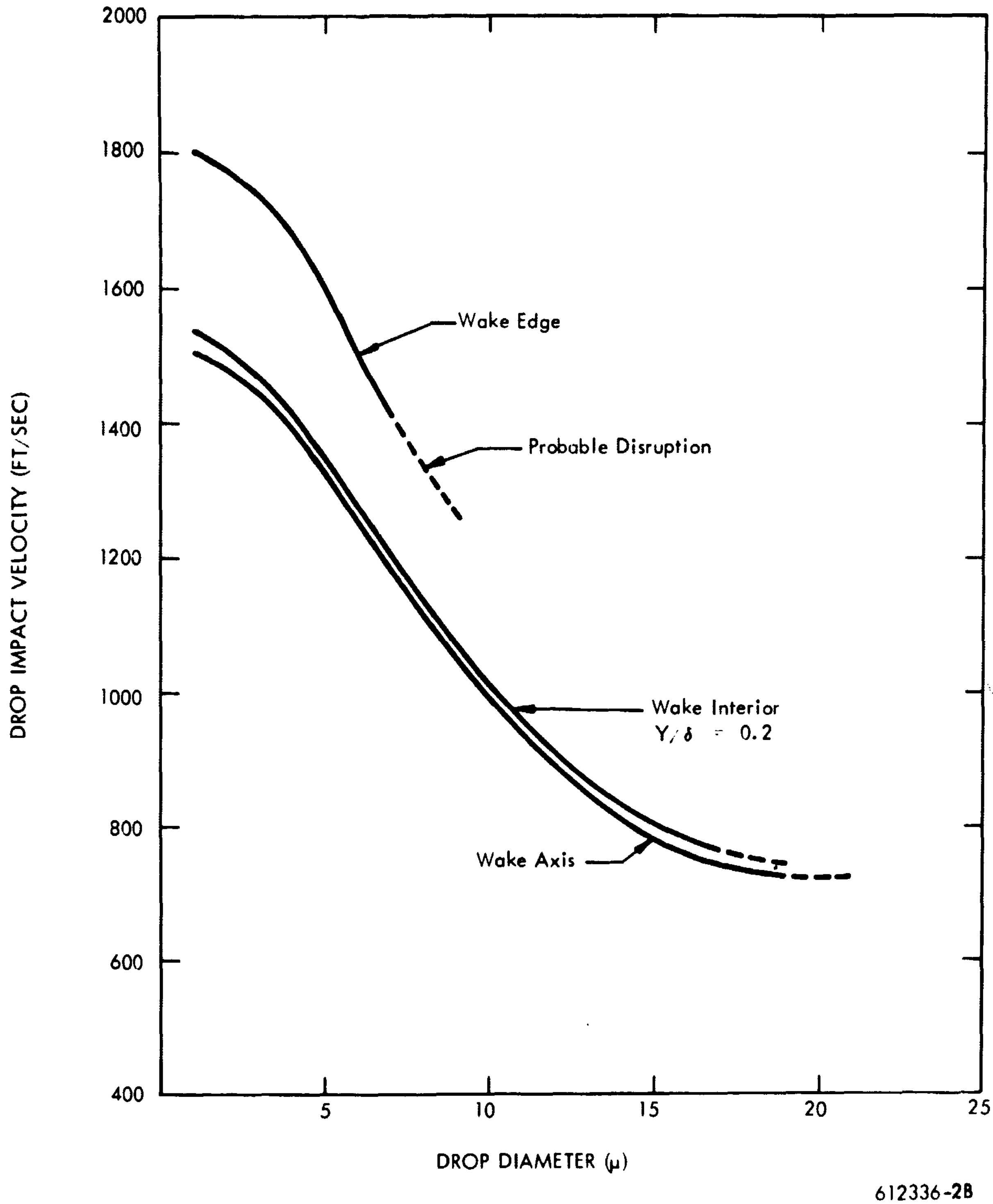

Figure 6. Estimated Drop Impact Velocities for the Final Rotor Section of the Five Stage Potassium Turbine.

6. PREDICTION OF DROPLET IMPACT VELOCITIES AND THE PHYSICAL EXTENT OF EROSION

In addition to the size of impacting droplets it is necessary to examine their velocities at impact to assess the amount and location of possible rotor blade erosion. The velocity triangles in Figure 7 indicate the geometric conventions used in this analysis. The drop velocity relative to the stator is given by:

$$W_d = \sqrt{U_1^2 + V_d^2 - 2 U_1 V_d \operatorname{Sin} \alpha} \tag{9}$$

The angle α_d satisfies:

$$\cos \alpha_d = \frac{U_1 - V_d \sin \alpha}{W_d} \tag{10}$$

The component of the drop velocity normal to the rotor blades is directly related to the degree of mechanical erosion. The normal velocity component is obtained by noting that the angle β included between W_d and W_n is $\pi/2 - \alpha_d - \alpha_i$. Therefore:

$$W_n = W_d \cos \beta = W_d \sin (\alpha_d + \alpha_i) \tag{11}$$

Depending on the angle of the blades and the angle of incidence of the droplets there will generally be a blade region which will be shadowed and free of damaging impacts. To estimate the extent of unshadowed blade surface a first approximation is to consider the "impaction length" ΔL defined (see Figure 7) along the tangent to the blade centerline at its nose. If the angles α_d and α_i are relatively acute the approximation is a relatively good one. Otherwise reasonable results may be obtained graphically if scale drawings of the blades are available. A relation for ΔL in terms of the blade spacing S and angles α_i and α_d is:

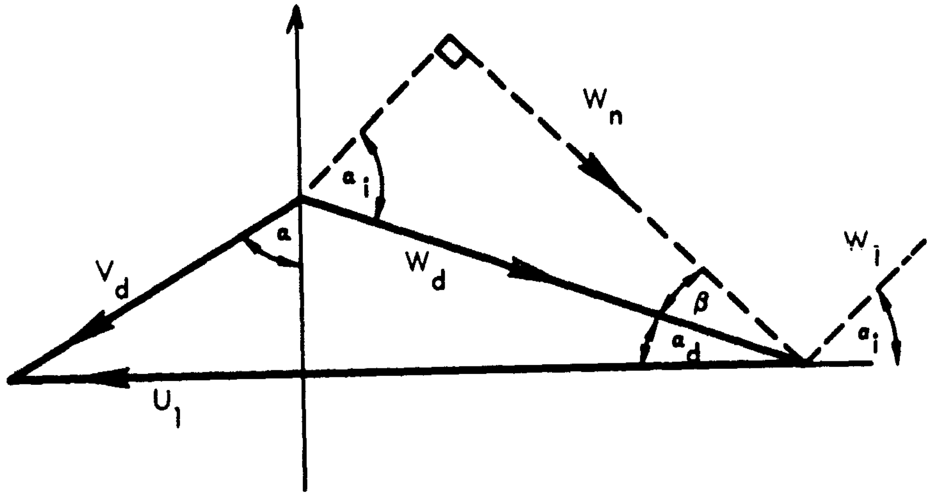

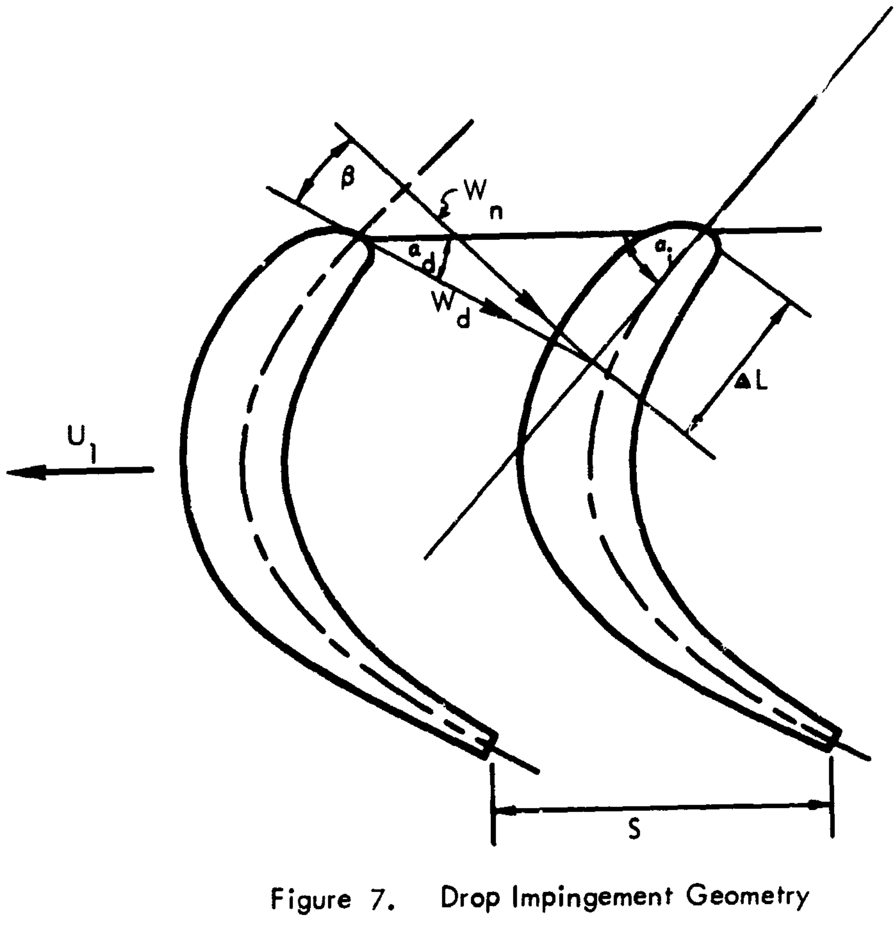

Figure 7. Drop Impingement Geometry

$$\Delta L \approx S \frac{\sin \alpha_d}{\sin (\alpha_i + \alpha_d)} \qquad (12)$$

Parametric data on impact velocities and lengths has been prepared for each stator of interest, covering the potential range of drop impact velocities. Figures 8 through 11 illustrate the variation of W_n, W_d and ΔL with velocity V_d, the final drop velocity relative to the stators at impact, for the four terminal rotors. Calculations were done with mean diameter blade properties.

The primary drop limit estimates made in the preceding section and listed in Table 7 may be used to establish lower limits to the range of V_d, drop impact velocity, in the above curves. It is evident that the normal component W_n is very small for all of the cases. Somewhere on the nose of the rotor blades, however, the vector W_d will be normal to the curved surface so that impact damage, if present at all, is expected to be greatest at that position.

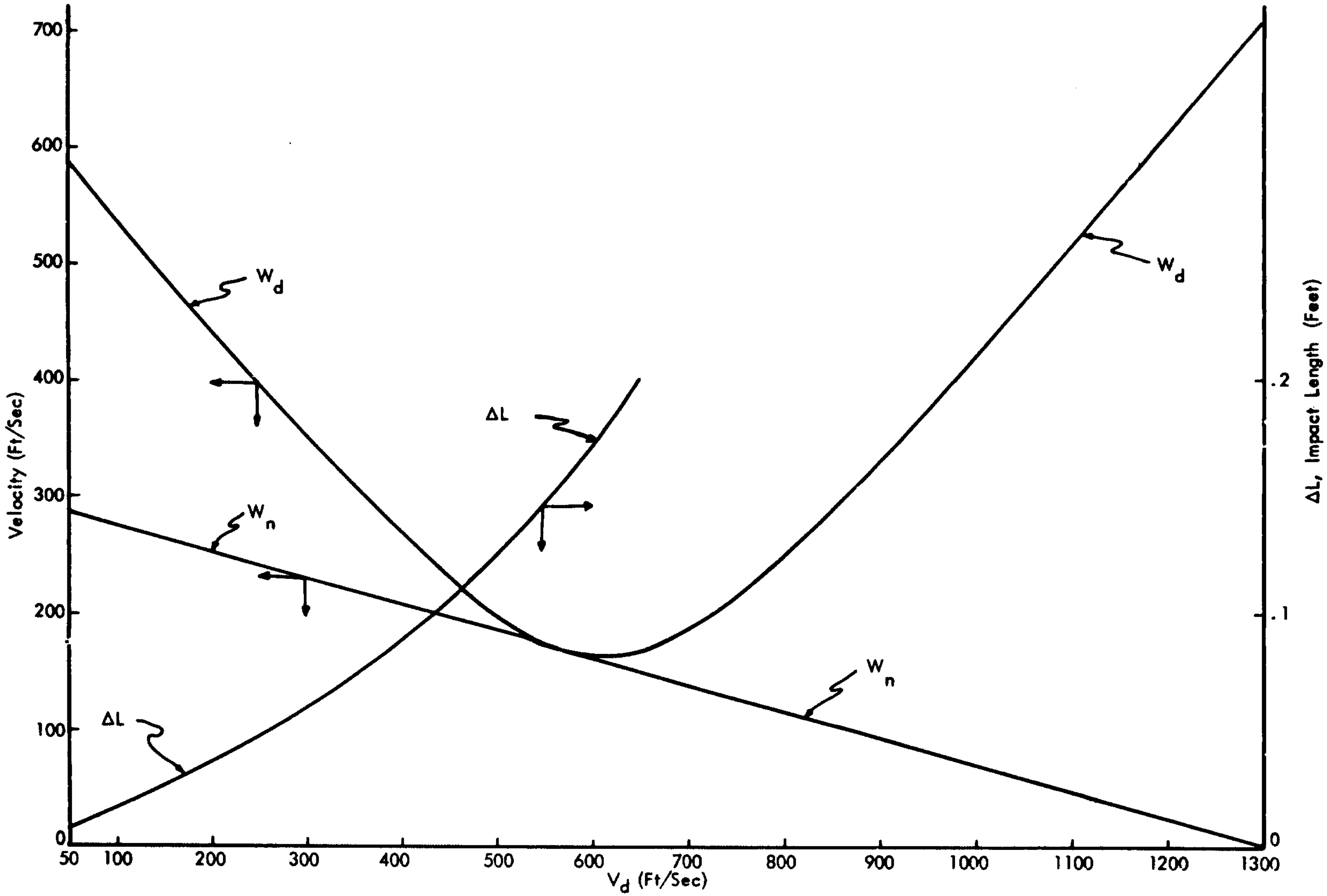

Figure 8. Normal Drop Impact Velocities for the 2-Cs Turbine

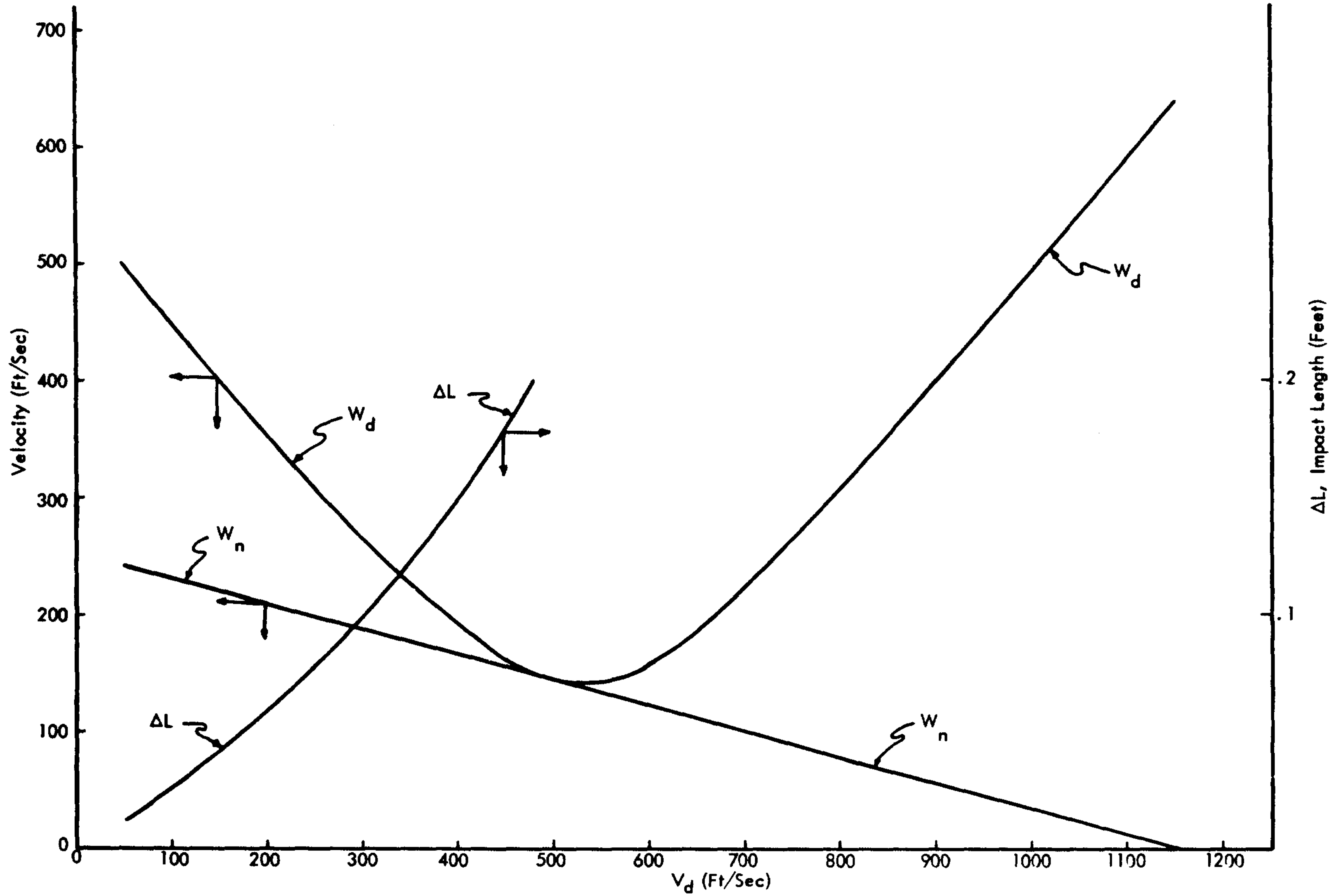

Figure 9. Normal Drop Impact Velocities for the 3-Cs Turbine

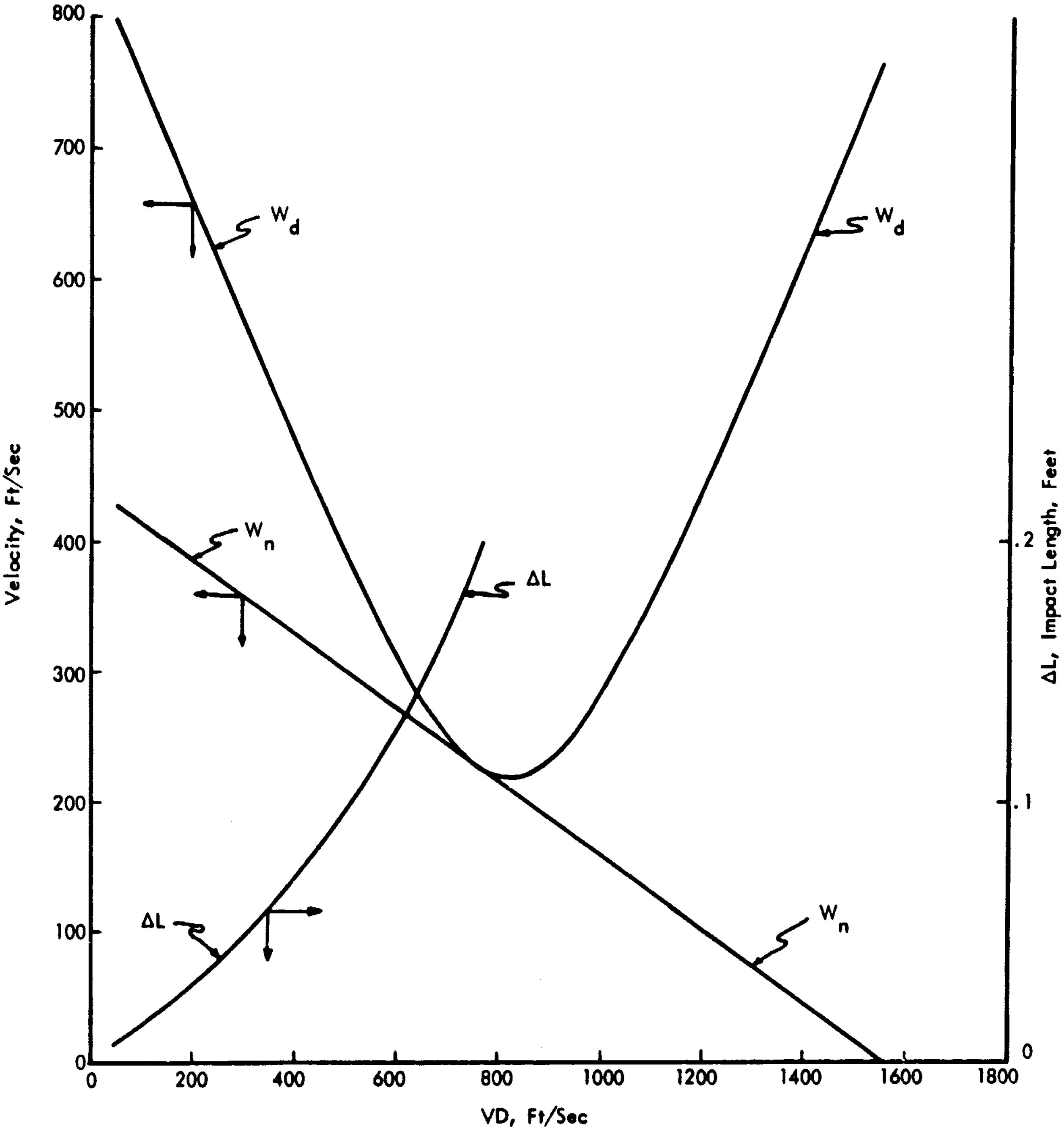

Figure 10. Normal Drop Impact Velocities for the 5-K Turbine

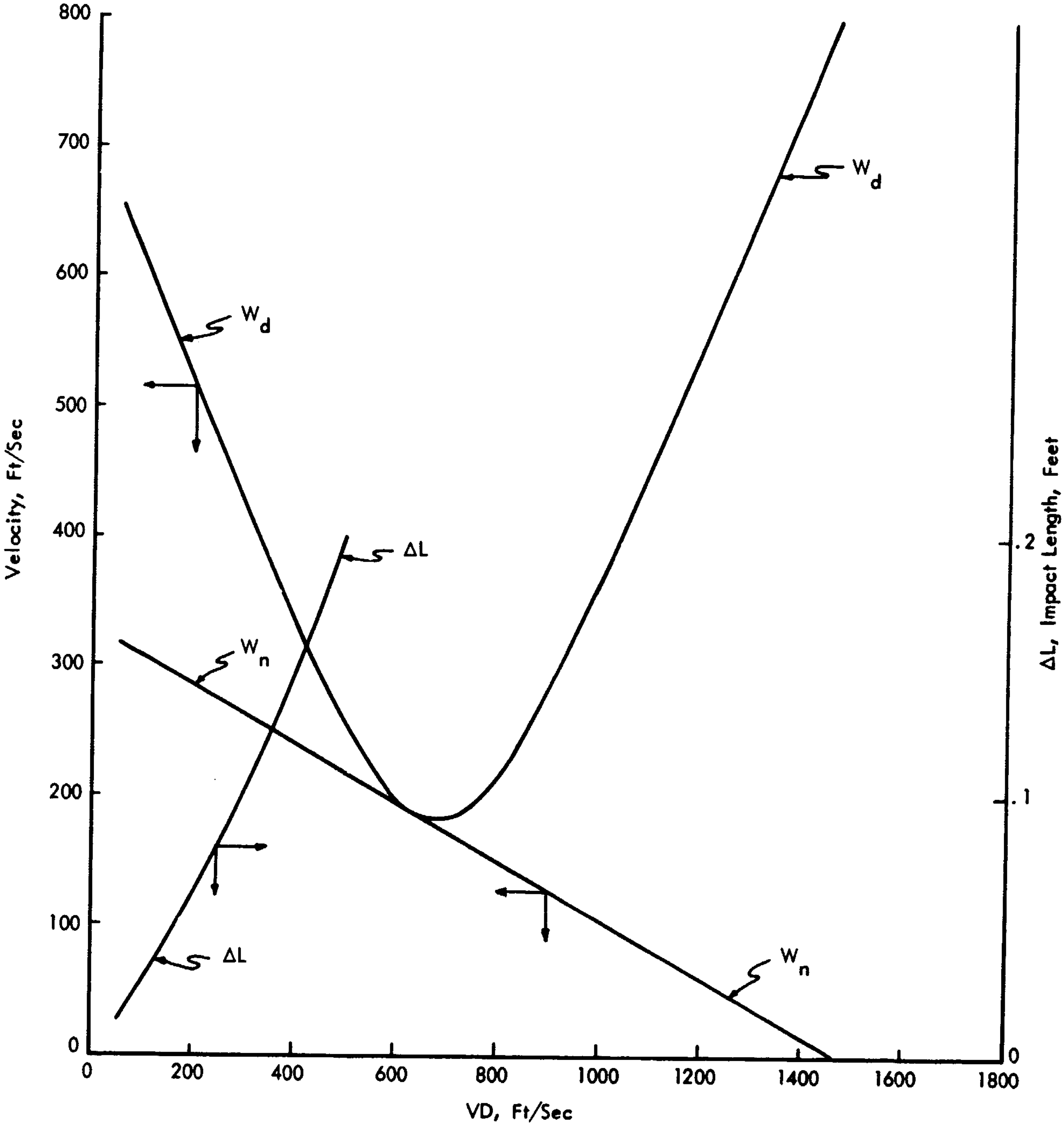

Figure 11. Normal Drop Impact Velocities for the 8-K Turbine

7. THRESHOLD VELOCITIES FOR MECHANICAL EROSION IN THE REFERENCE TURBINE SYSTEMS

A correlation has been proposed by Pouchot[10] to permit estimation of the damaging velocity threshold for rotor blade impacts. An important aspect of the correlation is the assumption of a liquid film on the rotor surface which acts to attenuate the force of drop impact. The thickness of the film is related in a consistent manner to the blade geometry and blade RPM. The threshold velocity is then a function of the drop liquid material properties, the drop size and film thickness, and a strength of material criterion. The criterion selected is the hardness of the blade material as measured in terms of the Vickers VPN.

Four different values of VPN were used to bracket potential bucket materials. These were:

VPN	Typical Material
190	12% Chrome Steel
260	TZM
400	Stellite 6
500	Maraging Steel

Table 8 summarizes our preliminary conclusions concerning the threshold velocities associated with the last row of rotor blades of the four turbines of interest. Design blade tip speeds have been used in this study. The threshold velocity decreases with increasing drop diameter. The primary drop size limits presented in Table 7 have been used in these estimates. In each case the threshold velocities are well above the maximum normal impact velocities which may be expected (see Figures 8 through 11). An exceedingly small number of the impacting drops will approach the limiting sizes quoted, so that from the classical mechanical erosion point of view very little blade damage is expected.

Table 8. Estimated Threshold of Damaging Impact Velocity for the Reference Turbine Systems

Turbine Stage	Primary Drop Diameter (μ)	Threshold Velocities (fps) for Various Values of VPN 190	260	400	500
2Cs - 2	1.	> 3000	> 3000	> 3000	> 3000
	5.	2876	> 3000	> 3000	> 3000
3Cs - 3	1.	> 3000	> 3000	> 3000	> 3000
	5.	> 3000	> 3000	> 3000	> 3000
5K - 5	8.	> 3000	> 3000	> 3000	> 3000
	20.	2083	2850	> 3000	> 3000
8K - 8	10.	> 3000	> 3000	> 3000	> 3000
	30.	1822	2493	> 3000	> 3000

8. CONCLUSIONS

Four liquid metal vapor turbine designs have been examined to determine their potential for turbine bucket erosion. Emphasis has been placed on those factors which we believe are most important from the classical mechanical erosion point of view. In this view blade damage is due to the prolonged impingement of liquid drops on rotor surfaces. The eroding moisture is that liquid which has collected on and discharged from the back end of preceding stators. The amount of erosion caused by this kind of mechanism is very particle size dependent. In fact there appears to be a threshold below which damage is negligible.

According to the interpretation of the erosion process upon which the erosion model is based the total quantity of impacted moisture is not significant provided one is operating below the erosion threshold. Estimates of the damaging drop velocity threshold appear to be far greater than expected impact velocities for all turbines considered. Limits for the largest size of primary drops expected to impact the rotors have been estimated. Cesium turbines are generally good atomizers so that even though their mass flow rates are greater than those in comparable potassium machines, the size of impacting drops is considerably less.

It is apparent therefore that whether or not moisture is removed between stages is of little consequence from the classical erosion viewpoint. There are, however, other justifications for this procedure. Chemical dissolution of blade materials and other surfaces may be reduced in this fashion and, in particular, the combined effects of selective leaching and mechanical impingement may be reduced to a negligible level.

Inter-stage moisture removal also appears to be important in the reduction of the liquid film which may accumulate along the walls of the turbine casing. This problem has been examined in detail in reference (9). Most of the moisture which impacts turbine rotors will eventually be centrifuged off onto the casing walls. There is evidence that part of this moisture will be returned to the vapor stream in the form of very large droplets. Excessive moisture accumulation of this sort may accelerate erosion of parts other than rotor blade surfaces, such as housing walls, seals, and moisture removal slots.

NOMENCLATURE

Symbol	Definition
a	Ellipse semi-minor axis
$\bar{D}$	Passage mean line diameter
$\bar{D}_I$	Stator inlet mean diameter
$\bar{D}_o$	Stator exit mean diameter
D_d	Drop diameter
L	Stator axial length
L'	Effective flow passage length
N_B	Number of blades per row
S	Pitch
U_1	Peripheral blade speed at a reference diameter
V_d	Droplet velocity with respect to stator
VPN	Vickers hardness number
V_{rel}	Relative velocity of drop with respect to the local vapor velocity
W_d	Droplet velocity relative to rotor
W_n	Normal component of droplet velocity relative to rotor
We_d	Droplet Weber Number
y, y'	Circumferential distance in the radial projection
Z	Axial distance (parallel to the turbine axis)
α	Flow angle for droplets torn off stator with respect to the axial direction
α_d	Angle between velocity W_d and tangential velocity U_1
α_i	Inlet flow angle to rotor with respect to tangential velocity U_1
β	Angle between velocities W_d and W_n
ΔL	Impaction length, i.e., the approximate length [illegible] blade which is not shadowed by other blades in the row
ρ_v	Density of liquid
σ_d	Drop surface tension

Symbol	Definition
$\delta_S, \ _p$	Boundary layer thickness on the suction and pressure sides
δ_S^*, δ_p^*	Boundary layer displacement thickness
θ_S, θ_S	Boundary layer momentum thickness

REFERENCES

1. Westinghouse Astronuclear Laboratory, "Analytical Investigation of Turbine Erosion Phenomena", Interim Technical Report No. 1, Vol. II, Contract NAS 7-390, November 1966.

2. R. E. Kothmann, "Condensation of Wet Vapors in Turbines", WANL-TME-1668, October 15, 1967.

3. R. E. Kothmann, "Basic Investigation of Turbine Erosion Phenomena", Quarterly Progress Report, WANL-PR(DD)-023, June 1967.

4. Katsanis, T., "A Computer Program for Calculating Velocities and Streamlines for Two-Dimensional Incompressible Flow in Axial Blade Rows", NASA-TN-D-3762, January 1967.

5. Lieblein, S., and Roudebush, W. H., "Low Speed Wake Characteristics of Two-Dimensional Cascade and Isolated Airfoil Sections", NACA-TN-3771, October 1956.

6. Fentress, W. K., "A Computer Program for Calculating the Boundary Layer Properties Along the Surface of Turbomachinery Blades", WANL-TME-1689, November 1967.

7. Fentress, W. K., "Analytical Investigation of Turbine Erosion Phenomena", Interim Technical Report, WANL-PR(DD)-014, Volume 2, Section C-4, November 1966.

8. Gardner, G. C., "Events Leading to Erosion in the Steam Turbine", Proc. Inst. Mech. Engrs., Vol. 178, Part 1: No. 23, pp 593 to 623, 1963-1964.

9. Westinghouse Astronuclear Laboratory, "Basic Investigation of Turbine Erosion Phenomena", Monthly Progress Report, WANL-PR(DD)-030, January 1968.

10. Pouchot, W. D., "Basic Investigation of Turbine Erosion Phenomena", Quarterly Progress Report, WANL-PR(DD)-020, Section 4, March 1967.